International Journal on Interactive Design and Manufacturing (IJIDeM) (2020) 14:345–357
https://doi.org/10.1007/s12008-019-00593-4

ORIGINAL PAPER

# Shrinkage prediction of injection molded high density polyethylene parts with taguchi/artificial neural network hybrid experimental design

**Rafa Abdul[1] · Gangjian Guo[1] · Joseph C. Chen[1] · John Jung-Woon Yoo[1]**

Received: 17 May 2019 / Accepted: 25 May 2019 / Published online: 1 June 2019
© Springer-Verlag France SAS, part of Springer Nature 2019

**Abstract**
Injection molding is classified as one of the economical manufacturing processes for high volume production of plastic parts. However, it is a complex process, as there are many factors that could lead to process variations and thus the quality issues of final products. One common quality issue is the presence of shrinkage and its associated warpage. Part shrinkage is largely affected by molding conditions, as well as mold design and material properties. The main objective of this paper is to predict the shrinkage of injection molded parts under different processing parameters. The second objective is to facilitate the setup of injection molding machine and reduce the need for trial and error. To meet these objectives, an artificial neural network (ANN) model was presented in this study, to predict the part shrinkage from the optimal molding parameters. Molding parameters studied include injection speed, holding time, and cooling time. A Taguchi-based experimental study was conducted, to identify the optimal molding condition which can lead to the minimum shrinkages in the length and width directions. A $L_{27}$ ($3^3$) orthogonal array (OA) was applied in the Taguchi experimental design, with three controllable factors and one non-controllable noise factor. The feedforward neural network model, trained in back propagation, was validated by comparing the predicted shrinkage with the actual shrinkage obtained from Taguchi-based experimental results. It demonstrates that the ANN model has a high prediction accuracy, and can be used as a quality control tool for part shrinkage in injection molding.

**Keywords** Injection Molding · Shrinkage · Artificial neural network · Taguchi methodology · Polyethylene

## 1 Introduction

Injection molding is a widely used process to shape thermoplastic materials into molded products of intricate shapes. It is particularly suitable for mass production due to its short cycle time and high tooling cost. The qualities of injection moldings are affected by many factors such as plastic part design, mold design, materials, and molding parameters. One of common quality issues for injection moldings is part shrinkage. Part shrinkage is natural due to thermal contraction, as the plastic material changes from its high temperature molten state to low temperature solid state, to form the desired shape in the mold cavity. A packing phase is thus required to force more plastic melt into the mold cavity to compensate for material shrinkage during mold cooling. Large non-uniform shrinkages, due to poor part or tooling design and improper molding conditions, often create internal or residual stresses that could lead to part warpage. Therefore, it is highly desirable to minimize the shrinkage of injection moldings by optimizing processing conditions, and to predict the shrinkage under different molding parameters. This will help reduce the setup time with proper molding parameters and improve the quality of injection moldings.

Shrinkage prediction for plastics injection molding has been studied extensively. Han et al. [1] developed a simulation program based on crystallization kinetics to predict the shrinkage of slowly-crystallizing thermoplastic polymers in injection molding. The material properties such as viscosity, thermal conductivity, heat capacity, PVT (pressure–volume-temperature) relation and crystallization kinetics were considered in their study. Jansen et al. [2] studied the effect of processing conditions on shrinkage for seven thermoplastic polymers, and concluded that a simple thermoelastic model used in the study could predict amorphous polymers, but it

✉ Gangjian Guo
gguo@fsmail.bradley.edu

[1] Department of Industrial & Manufacturing Engineering & Technology, Bradley University, Peoria, IL 61625, USA

over-predicted for semi-crystalline polymers. Choi et al. [3] conducted a numerical analysis of shrinkage for amorphous polymers in consideration of the residual stresses produced during the packing and cooling stages of injection molding. These shrinkage predictions with conservation equations (mass, momentum and energy) are associated with assumptions and simplifications to obtain the solutions. Some commercial simulation programs such as Moldflow were used for predicting the shrinkage. Lucyshyn et al. [4] used a differential scanning calorimeter to identify the transition temperatures at different cooling rates, and applied the transition temperatures in calculating the shrinkage with Moldflow. Pomerleau et al. [5] investigated the injection molding shrinkage of polypropylene with a factorial design of experiment, and examined the effects of holding pressure and injection velocity on shrinkages.

Artificial neural network (ANN) is a modeling technique that is capable of dealing with highly nonlinear problems with multi-input and multi-output systems. It requires no assumption of the problem and has a strong adaptive learning capability. ANN handles information in a way similar to the operation mechanism of neurons within the human brain. It has been applied to various applications such as design optimization, pattern recognition, etc. In the literature, there are a few studies that applied ANN in injection molding to predict part shrinkage. Shen et al. [6] used the combination of ANN and genetic algorithm (GA) to optimize the injection molding process for minimizing the volumetric shrinkage variation. Lee et al. [7] developed a neural network which was trained by the data from a numerical flow analysis, to predict shrinkage of the injection molded polypropylene parts. Liao et al. [8] demonstrated the successful use of back-propagation ANN in predicting the shrinkage and warpage of injection-molded thin-wall parts, and amorphous plastics polycarbonate and acrylonitrile butadiene styrene were used in their study. Wang et al. [9] evaluated the effect of injection molding process parameters on shrinkage based on neural network simulation, however, the data input was from Moldflow simulation results and no real experiments were conducted. Altan et al. [10] reduced shrinkage in injection moldings via the Taguchi, ANOVA and neural network methods for PP and polystyrene (PS). The same network was used to predict both PP and PS. Tsai et al. [11] combined the ANN with a genetic algorithm (GA) to establish an inverse model of injection molding for optical lens form accuracy.

High density polyethylene (HDPE) is one of the most widely used thermoplastics in injection molding, because it offers many benefits such as low processing temperature, low cost, good stiffness and toughness, compared to other thermoplastics. As a semi-crystalline polymer, HDPE typically has a higher shrinkage than amorphous plastics, due to its higher crystallinity. The Taguchi approach has been used to optimize injection molding conditions to achieve desirable product qualities [10–13]. Compared with a factorial design, the Taguchi approach is more efficient with a fewer resources required.

To our knowledge, few studies have been conducted to investigate the shrinkage prediction accuracy of injection molded HDPE parts by using the combination of ANN and the Taguchi approach. In this study, back propagation ANN is used as data-driven modeling technique in predicting the minimum shrinkages along the flow direction (i.e., the length) and the cross-flow direction (i.e., the width), under the injection molding conditions optimized by the Taguchi approach. Three important molding parameters studied include injection speed, holding time, and cooling time. A Taguchi orthogonal array ($L_{27}$) was designed for conducting experiments, to identify the optimal molding conditions for minimum shrinkages. Experimental data were used to train, test, and validate the ANN model. The main objective is to predict the minimal shrinkage under the optimized molding parameters. The second objective is to facilitate the molding setup with proper molding parameters and reduce the need for trial and error.

## 2 Model description

### 2.1 ANN

Figure 1 shows the typical structure of ANN. It consists of an input layer, hidden layer(s), and an output layer. Each layer has several elements which are called nodes or neurons. The links between elements carry values (or weights), and they usually determine the network function. ANN is trained by adjusting the link weights to perform a particular function for reaching the target outputs. Many input/target data pairs are required to train a network [14]. In this study, we have three inputs (injection speed, holding time, and cooling time) and two outputs (length and width shrinkages).

### 2.2 Multi-layer ANN and backpropagation training

For the feedforward model adopted in this study, there are three neurons in its input layer, which are the dimensionless injection speed, cooling time and holding time. The output layer has two neurons, which are the length shrinkage and width shrinkage. Experimental data are randomly separated into a training set, a testing set, and a validation set. The training set is used to train the backpropagation ANN to identify the relationship between the inputs and the outputs. The testing set is used to test the prediction performance of the ANN. There were 27 experimental data points used to train the ANN. The number of hidden layers, the transfer function of hidden layer, the learning rate, the minimum gradient and momentum are considered in this study. The

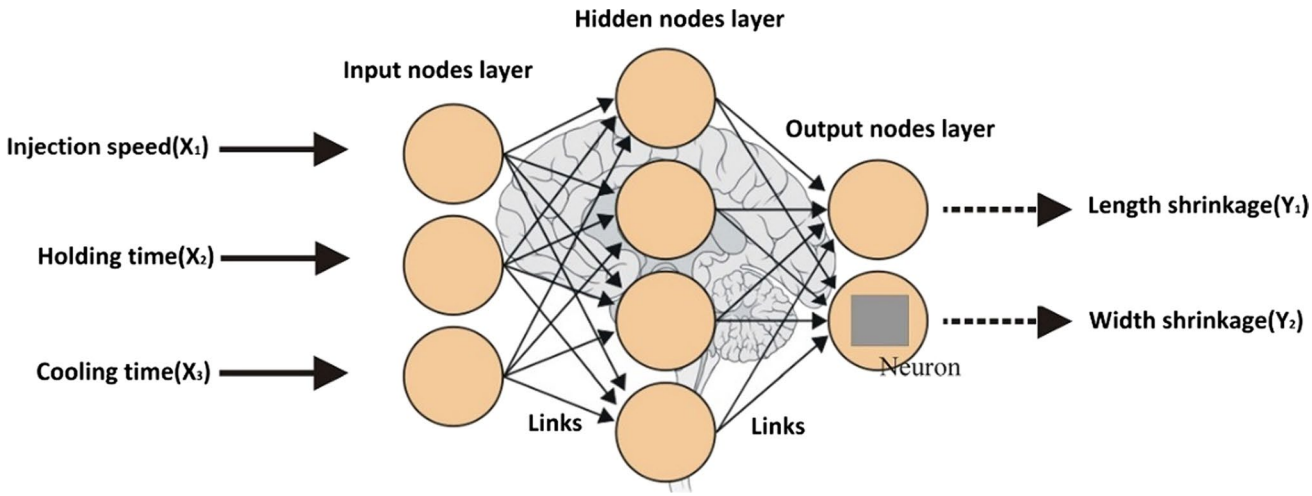


**Fig. 1** Typical structure of an ANN

training process for the ANN is stopped when one of two following criteria is met: (1) the sum squared error (SSE) should be smaller than 0.0001, and (2) the iteration epoch reaches 10,000 times. The training quality is determined by the root mean squared (RMS) error. The definitions of SSE and root mean squared error are [8]:

$$SSE = \sum_{j=1}^{m} \sum_{i=1}^{n} (Tij - Pij)\text{^}2$$
$$RMS_q = \sqrt{\frac{SSEq}{m \times n}} \tag{1}$$

where Tij is the target value, and Pij is the predicted value from the model.

### 2.3 Steps for the backpropagation ANN design process

The multilayer feedforward neural network is widely used for function fitting, pattern recognition, and prediction problems. In this study, the work flow for designing the feedforward ANN involves the following six primary steps:

1. Performing injection molding experiments and collecting the data set of inputs and outputs
2. Providing these input and output data pairs to the software (i.e., MATLAB-Mathworks)
3. Tagging the data as inputs, outputs, training, and testing
4. Creating a custom network of the required structure (check for the network with the least RMSE value)
5. Training and testing the network, checking for the least RMSE value. The data tagged as "train" will be used for training;
6. Validating the network with the validating data set for post-training analysis
7. Using the network for predicting the minimum shrinkages under the optimal molding condition.

## 3 Experimental

### 3.1 Molding machine and experimental material

The molding machine used is Engel E-victory 30 with a clamping force of 30 ton, and it has the screw diameter of 22 mm and the L/D ratio of 30. HDPE (Proline 2053), supplied by Shannon Industrial Corporation, has a density of 0.953 g/cm$^3$ and a melt flow index of 18 g/10 min.

### 3.2 Mold design

A two-part family mold was designed as shown in Fig. 2. The fan gate was selected to achieve a uniform material flow, minimize backfilling and part warpage, and keep the cross sectional area constant. The steel insert mold base, from DME Company (Model 08/09 U Style Frame), was cut with a CNC machining center. The original length and width of the mold cavity are 116.56 mm and 19.25 mm, respectively, measured with a coordinate measuring machine (CMM, Mitutoyo). The resolution of CMM is 0.0005 mm. All the injection molded samples were measured with the CMM.

The length and width shrinkages were calculated as follows.

$$S_L = (L_m - L_p)/L_m \times 100\%$$
$$S_W = (W_m - W_p)/W_m \times 100\% \tag{2}$$

where $S_L$ = length shrinkage, $L_m$ = mold length, $L_p$ = part length, $S_w$ = width shrinkage, $W_m$ = mold width, $W_p$ = part width

**Fig. 2** The mold used in the study

### 3.3 Baseline study

The baseline study was conducted with the injection speed 10 $cm^3/s$, the injection pressure of 1000 bar, the cooling time of 24 s, and the holding time of 14 s. The obtained average length shrinkage and width shrinkage from the baseline study were 2.64% and 3.56%, respectively.

## 4 Results and discussions

### 4.1 Taguchi experimental design

The Taguchi method was applied to identify the effects of the molding parameters on the flow direction shrinkage (i.e., length shrinkage) and the cross flow shrinkage (i.e., width shrinkage). The optimum molding condition for the minimum shrinkages can be obtained through the Taguchi experiments. Similar to the ANN, the three significant controllable molding parameters with three levels were selected, as shown in Table 1. The output variables are the length and width shrinkage. The environment temperatures, the room temperature without ventilation (70 °F) and the room temperature with ventilation (65 °F), were selected as the noise factor. The measured shrinkage values and the signal-to-noise (S/N) results are given in Table 1. Each row in the table represents an experiment with different combination of molding parameters and their levels. However, these experiments were conducted randomly. The S/N ratio is a quality indicator that is used to evaluate the effects of the molding parameters on the shrinkages of the injection moldings. In this study, ‘‘the smaller the better” criterion was selected when calculating the S/N ratios, as minimizing the shrinkages is the goal.

$$\eta = \frac{\mathrm{S}}{\mathrm{N}} = -10\mathrm{Log}\left(\sum_{i=1}^{n} Yi^2 \Big/ n\right) \tag{3}$$

where η is the S/N ratio, $Y_i$ is the individual shrinkage measurement, and n is the number of measurements for each run.

### 4.2 Analysis of noise factor and S/N ratio for the length and width shrinkages

Table 2 is the response table for the mean length and width shrinkages, as well as their associated S/N ratios. The table is used to determine the optimal combination of the controllable factors that leads to the minimum shrinkage. Figure 3 shows the graphical representation of the effects of molding parameters on the shrinkage and S/N ratio. Since the shrinkage is the-smaller-the-better, the optimal setting combination for the minimum length shrinkage is $A_2$-$B_1$-$C_3$, which is interpreted as the 2nd level of injection speed, the first level of holding time, and the third level of cooling time. For the S/N ratio, we are looking for the largest value. Therefore, the optimal setting combination for the S/N ratio of the length shrinkage is $A_2$-$B_3$-$C_3$. Similarly, the optimal setting combination for the minimum width shrinkage is $A_1$-$B_2$-$C_1$, and the optimal setting combination for S/N ratio of the width shrinkage is $A_3$-$B_3$-$C_2$.

### 4.3 Hypothesis testing for the length and width shrinkage

Table 3 shows the t-tests with 99% confidence level were conducted to determine if the environment temperature had a significant effect on the length and width shrinkages.

Based on the results, we fail to reject the null hypothesis, as the T value obtained is less than the T- critical value. Therefore, the length shrinkage and the width shrinkage are not significantly affected by the environment temperature.

### 4.4 Training and testing ANN

The training function (TRAINGDX), the adaptive learning function (LEARNGD), the performance function (MSE), and the transfer function (LOGSIG), are used in the back propagation ANN. They can be found in neural network toolbox [14]. In this study, 135 experimental data sets (see Appendix A) were used for training and testing the ANN. The inputs of the ANN include injection speed, holding time and cooling time, and the outputs are the width shrinkage and the length shrinkage.

**Table 1** Taguchi experimental design and results for length and width shrinkage (%)

| Test no. | Injection speed ($cm^3/s$) | Holding time (s) | Cooling time (s) | Room temperature without ventilation | | Room temperature with ventilation | | Y bar | | S/N ratio | |
|---|---|---|---|---|---|---|---|---|---|---|---|
| | | | | Length | Width | Length | Width | Length | Width | Length | Width |
| T-101 | 8(1) | 12(1) | 18(1) | 2.66 | 3.13 | 2.27 | 2.44 | 2.47 | 2.79 | −21.95 | −18.13 |
| T-102 | 8(1) | 12(1) | 24(2) | 2.56 | 2.65 | 2.47 | 2.92 | 2.52 | 2.78 | −35.48 | −26.50 |
| T-103 | 8(1) | 12(1) | 30(3) | 2.70 | 3.07 | 2.02 | 3.35 | 2.36 | 3.21 | −16.92 | −27.31 |
| T-104 | 8(1) | 15(2) | 18(1) | 3.14 | 3.02 | 2.69 | 3.14 | 2.92 | 3.08 | −22.31 | −34.40 |
| T-105 | 8(1) | 15(2) | 24(2) | 2.78 | 2.97 | 2.55 | 3.11 | 2.66 | 3.04 | −27.51 | −32.45 |
| T-106 | 8(1) | 15(2) | 30(3) | 2.69 | 3.87 | 3.07 | 1.90 | 2.88 | 2.89 | −23.78 | −9.80 |
| T-107 | 8(1) | 18(3) | 18(1) | 2.55 | 3.01 | 2.59 | 2.64 | 2.57 | 2.83 | −42.68 | −23.74 |
| T-108 | 8(1) | 18(3) | 24(2) | 2.65 | 3.36 | 2.93 | 2.56 | 2.79 | 2.96 | −26.22 | −17.48 |
| T-109 | 8(1) | 18(3) | 30(3) | 2.67 | 2.97 | 2.45 | 2.85 | 2.56 | 2.91 | −27.51 | −33.81 |
| T-110 | 10(2) | 12(1) | 18(1) | 3.07 | 3.42 | 2.29 | 4.04 | 2.68 | 3.73 | −16.87 | −21.70 |
| T-111 | 10(2) | 12(1) | 24(2) | 2.59 | 3.57 | 2.93 | 2.63 | 2.76 | 3.10 | −24.10 | −16.46 |
| T-112 | 10(2) | 12(1) | 30(3) | 2.71 | 4.39 | 2.23 | 4.42 | 2.47 | 4.40 | −20.32 | −49.13 |
| T-113 | 10(2) | 15(2) | 18(1) | 2.67 | 4.07 | 2.71 | 2.85 | 2.69 | 3.46 | −41.79 | −15.21 |
| T-114 | 10(2) | 15(2) | 24(2) | 2.51 | 2.34 | 2.02 | 4.04 | 2.27 | 3.19 | −19.47 | −11.77 |
| T-115 | 10(2) | 15(2) | 30(3) | 2.93 | 3.06 | 2.69 | 4.38 | 2.81 | 3.72 | −27.34 | −15.16 |
| T-116 | 10(2) | 18(3) | 18(1) | 2.75 | 4.07 | 2.55 | 3.10 | 2.65 | 3.59 | −28.33 | −17.46 |
| T-117 | 10(2) | 18(3) | 24(2) | 3.14 | 3.49 | 2.12 | 4.28 | 2.63 | 3.89 | −14.43 | −19.89 |
| T-118 | 10(2) | 18(3) | 30(3) | 2.60 | 3.83 | 2.23 | 1.60 | 2.42 | 2.71 | −22.41 | −8.40 |
| T-119 | 12(3) | 12(1) | 18(1) | 2.69 | 2.96 | 2.55 | 2.56 | 2.62 | 2.76 | −31.33 | −23.03 |
| T-120 | 12(3) | 12(1) | 24(2) | 2.66 | 4.04 | 2.65 | 2.97 | 2.65 | 3.51 | −67.73 | −16.39 |
| T-121 | 12(3) | 12(1) | 30(3) | 2.65 | 2.56 | 2.67 | 4.01 | 2.66 | 3.28 | −48.99 | −13.32 |
| T-122 | 12(3) | 15(2) | 18(1) | 2.76 | 2.85 | 2.68 | 4.04 | 2.72 | 3.44 | −37.67 | −15.40 |
| T-123 | 12(3) | 15(2) | 24(2) | 2.79 | 4.04 | 2.17 | 3.33 | 2.48 | 3.68 | −18.14 | −20.43 |
| T-124 | 12(3) | 15(2) | 30(3) | 2.66 | 2.63 | 2.64 | 3.18 | 2.65 | 2.9 | −50.13 | −20.46 |
| T-125 | 12(3) | 18(3) | 18(1) | 2.65 | 4.42 | 2.58 | 2.92 | 2.62 | 3.67 | −38.26 | −13.99 |
| T-126 | 12(3) | 18(3) | 24(2) | 2.76 | 2.85 | 3.12 | 5.72 | 2.94 | 4.28 | −24.28 | −9.96 |
| T-127 | 12(3) | 18(3) | 30(3) | 2.79 | 4.04 | 2.26 | 3.09 | 2.52 | 3.56 | −19.70 | −17.58 |

**Table 2** Response table for the mean length and width shrinkages and S/N ratios

| | Level | A (injection speed) | B (holding time) | C (cooling time) |
|---|---|---|---|---|
| Mean length shrinkage (%) | 1 | 2.64 | 2.58 | 2.66 |
| | 2 | 2.60 | 2.67 | 2.63 |
| | 3 | 2.65 | 2.64 | 2.59 |
| S/N ratio for length shrinkage | 1 | −27.15 | −31.52 | −31.24 |
| | 2 | −23.90 | −29.79 | −28.60 |
| | 3 | −37.36 | −27.09 | −28.57 |
| Mean width shrinkage (%) | 1 | 2.94 | 3.28 | 3.26 |
| | 2 | 3.53 | 3.27 | 3.38 |
| | 3 | 3.46 | 3.45 | 3.29 |
| S/N ratio for width shrinkage | 1 | −24.85 | −23.55 | −20.34 |
| | 2 | −19.46 | −19.45 | −19.04 |
| | 3 | −16.73 | −18.03 | −21.66 |

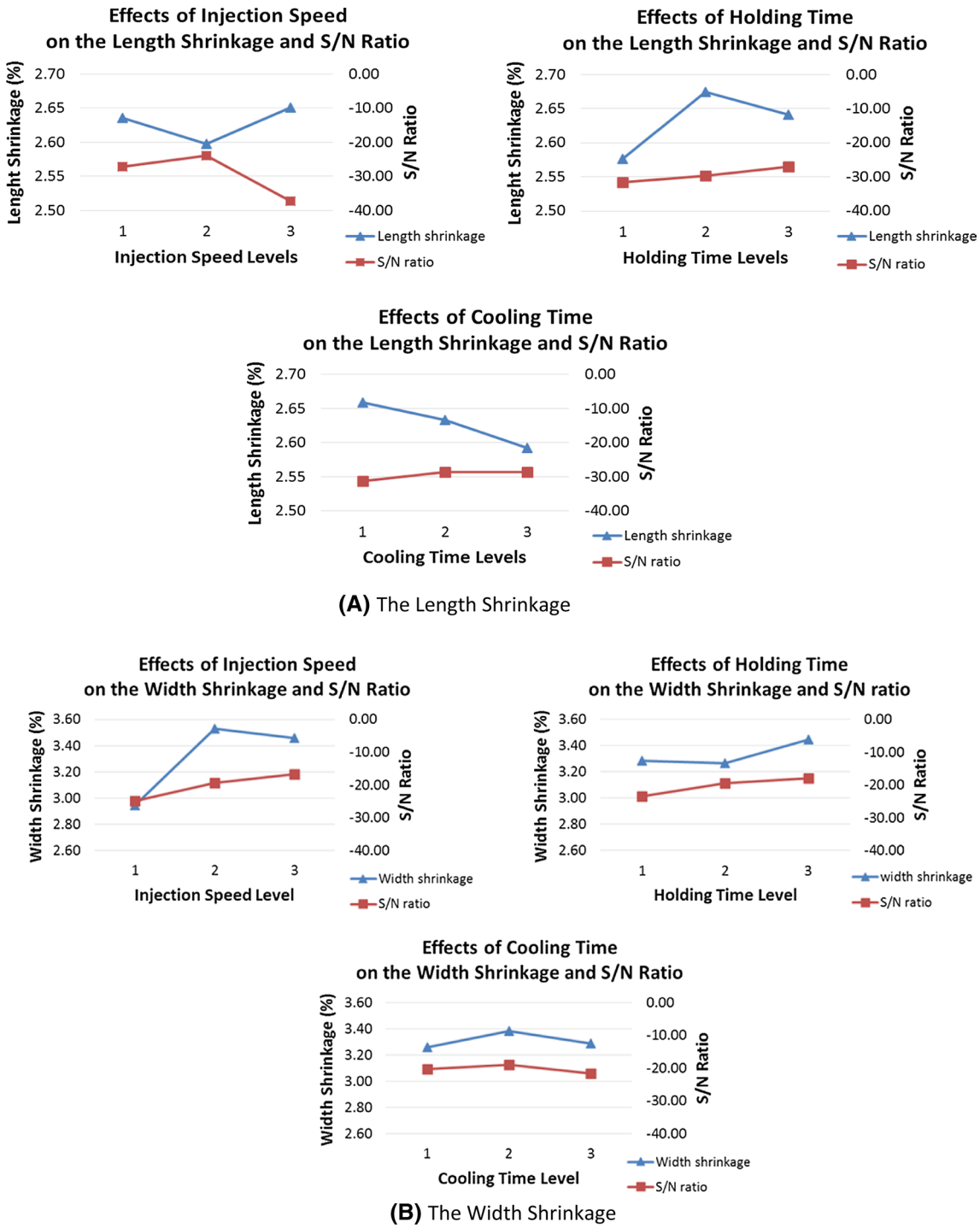


**Fig. 3** The main effect plots for **a** the length shrinkage; **b** the width shrinkage

**Table 3** T-test for the environment temperature effect on the length and width shrinkages

| | Length | Width |
|---|---|---|
| Average- room temperature without ventilation | 2.73 | 3.36 |
| Average- room temperature with ventilation | 2.52 | 3.26 |
| Variance—room temperature without ventilation | 0.026699 | 0.357715 |
| Variance—room temperature with ventilation | 0.088832 | 0.764972 |
| T value | 1.83 | 0.27 |
| Degrees of freedom | 79 | 79 |
| T-critical | 2.37 | 2.37 |
| Alpha | 0.01 | 0.01 |

Hypothesis: $H_0$: $\mu_{\text{room temperature without ventilation}} = \mu_{\text{room temperature with ventilation}}$, $H_1$: $\mu_{\text{room temperature without ventilation}} \neq \mu_{\text{room temperature with ventilation}}$

### 4.5 ANN network architecture

An optimum number of hidden layer neurons needs to be designed to accurately predict the outputs via the ANN. The best approach in seeking the optimum number of neurons is to first take a small number of neurons and then slightly increase it until a considerable improvement is observed. At the starting point of the process, 9 neurons was selected for the hidden layer. Then, the number of neurons increased every step. For the network structure, the selection of hidden layers is based on trial and error, and this study used one hidden layer. Finally, it was found that the 3-9-2-2 network structure has the least RMS error among all selected network structures. Thus, the 3-9-2-2 network structure, as shown in Fig. 4, was used in this study.

To train a multilayer network, the experimental data used is usually divided into three subsets. The first subset is the training set used for computing the gradient, the network weights, and the biases. The second subset is the validation set. The network weights and biases are saved at the minimum validation error. The third subset is the testing set used to compare different models. In this study, a total experimental set of 135 data samples, were used for the training, testing, and validation phases of the network models. The data subsets of training, testing, and validation were achieved by dividing roughly the available data set into 80, 15, and 5%, respectively.

### 4.6 Analyze neural network performance after training

Figure 5 shows the regression plots. It displays the network outputs (shrinkage) with respect to targets for training, validation, and test sets. If the R-value is equal to 1, that means the output is equal to the target. A larger R-value indicates a smaller difference between the output and the target. For this study, all the R-values are larger than 0.91, which means the fit is realistically good for all data sets. The minimal shrinkage was achieved with the highest R-value based on the training, validation, and testing errors. The analysis shows that the designed network (3-9-2-2) for the shrinkage parameter is sufficiently accurate. If more accurate results are required, the network can be retrained, or increased the number of hidden neurons, or applied different training functions, or improved with additional training data.

The validation set is used for tuning the model parameters. To make sure the network is not overfit, the validation set is used to check if the error is within some range.When the error in the measurement begins to increase, the training process must be stopped by the independent validation set. Figure 6 indicates the iteration at which the best validation performance reached a minimum at epoch 37. Figure 6 does not indicate any major problems with the training.

### 4.7 Comparison of prediction performance of ANN and the Taguchi methodology

Table 4 show the prediction performance of the ANN and the Taguchi experimental data for the length and width shrinkage under the optimal molding conditions. It indicates that the ANN model can predict the shrinkages that are very close to the Taguchi experimental data. Figure 7 shows the comparison of the experimental data and the ANN predicted data for randomly selected 27 test pairs. It demonstrates that the ANN model has a high prediction accuracy.

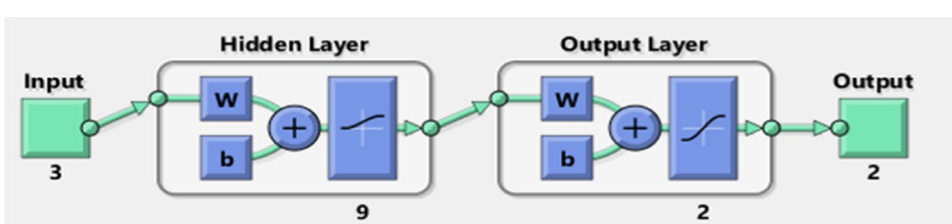


**Fig. 4** The ANN network architecture

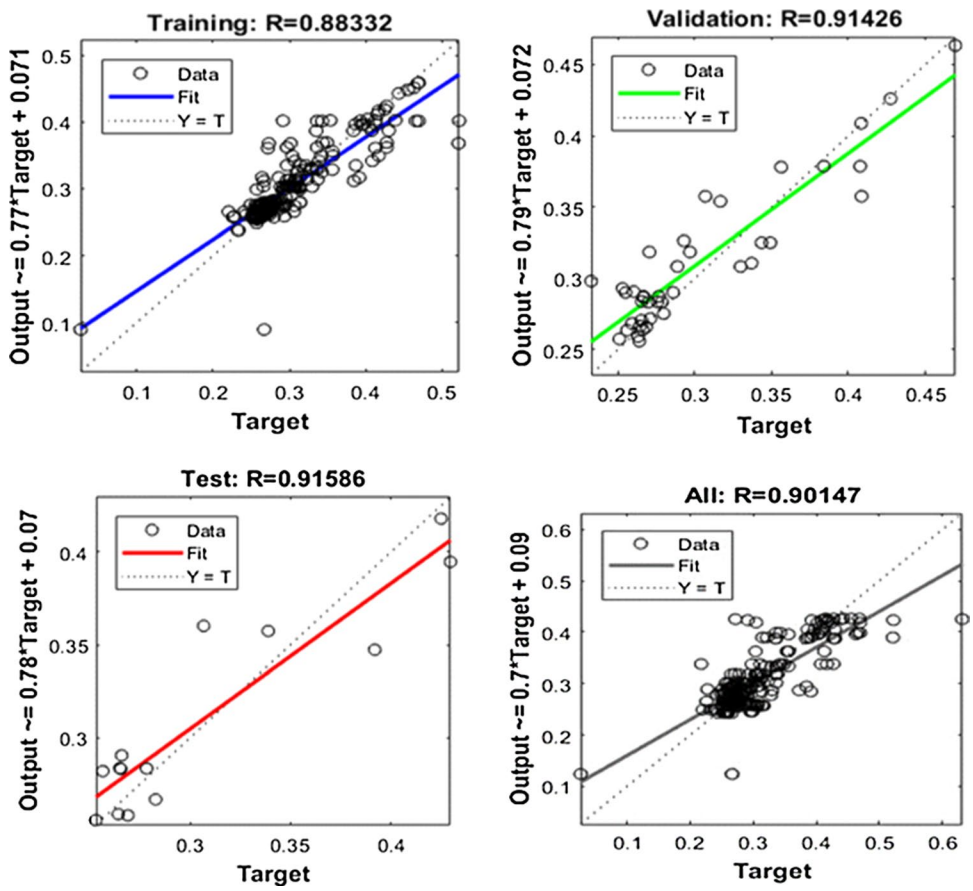


**Fig. 5** R-value for testing, training, and validation

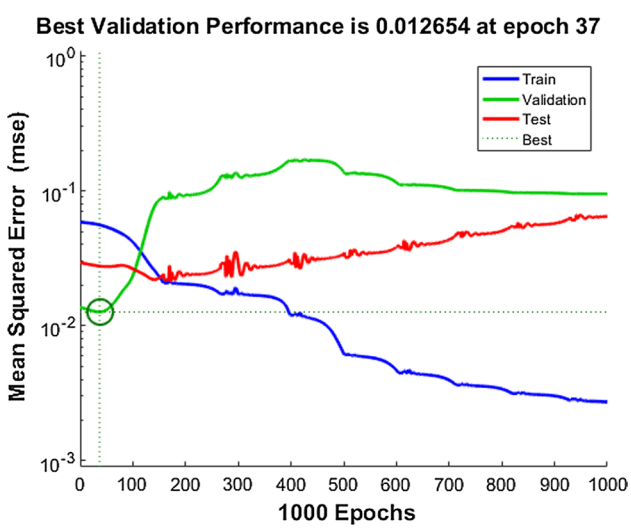


**Fig. 6** Schematic representation of validation performance

## 5 Conclusion

In this study, the Taguchi approach and the ANN model were utilized to investigate the effects of injection speed, holding time, and cooling time on the length shrinkage and the width shrinkage of HDPE injection moldings. The experimental results indicate that all these selected factors have significant effects on the shrinkages. The best combination of molding parameters for the minimum shrinkages was identified through the Taguchi experiments. Compared with the shrinkages obtained from the baseline experiments, the length shrinkage and the width shrinkage under the optimal molding conditions were reduced by 5.06% and 20.4%, respectively. A multi-layer feedforward ANN was designed, backpropagation trained, tested and validated with the experimental results. It turned out that the ANN model has a similar prediction performance under the optimal

**Table 4** Length and width shrinkage comparison: experimental versus ANN prediction

| Optimal process conditions | Experimental (Taguchi) (%) | Neural network prediction (%) | Error (%) |
|---|---|---|---|
| Length Shrinkage under $A_2$–$B_1$–$C_3$ condition | 2.5083 | 2.5062 | 0.08 |
| Width Shrinkage under $A_1$–$B_2$–$C_1$ condition | 2.8353 | 2.8155 | 0.69 |

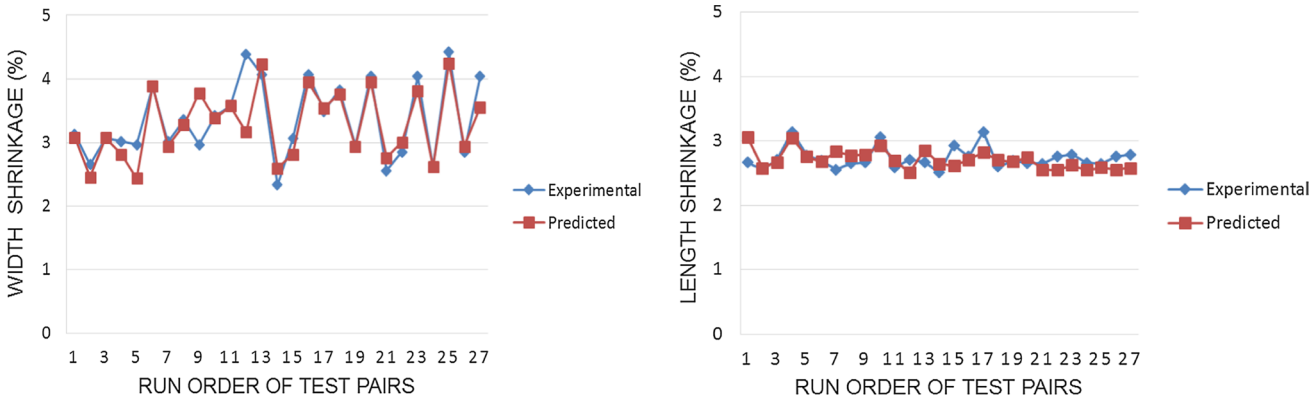


**Fig. 7** Width and length shrinkages: experimental versus predicted values

molding conditions for minimal shrinkages, compared with that of the Taguchi approach. In addition, the comparison of the experimental data and the ANN predicted data for randomly selected 27 test pairs under different molding conditions indicates that the ANN model has a high prediction accuracy. The combined use of the Taguchi approach and the ANN model, demonstrated in this study, would provide an efficient and effective way for injection molders to predict and minimize the shrinkages along the flow direction and the cross-flow direction under the optimal molding conditions, and to facilitate the molding setup and improve the quality of injection moldings.

**Funding** This research did not receive any specific grant from funding agencies in the public, commercial, or not-for-profit sectors. However, the corresponding author appreciates the Caterpillar Fellowship supported from Bradley University.

## Compliance with ethical standards

**Conflict of interest** All the authors of this paper do not have any conflicts of interest.

## Appendix

See Table 5.

**Table 5** Experimental data set used for the ANN training & testing

| Test no. | Injection speed ($cm^3/s$) | Holding time (s) | Cooling time (s) | Length shrinkage (%) | Width shrinkage (%) |
|---|---|---|---|---|---|
| T-101 | 8(1) | 12(1) | 18(1) | 2.66 | 3.13 |
| T-102 | 8(1) | 12(1) | 18(1) | 2.67 | 3.13 |
| T-103 | 8(1) | 12(1) | 18(1) | 2.65 | 3.14 |
| T-104 | 8(1) | 12(1) | 18(1) | 2.67 | 3.14 |
| T-105 | 8(1) | 12(1) | 18(1) | 2.66 | 2.65 |
| T-106 | 8(1) | 12(1) | 24(2) | 2.56 | 2.66 |
| T-107 | 8(1) | 12(1) | 24(2) | 2.66 | 2.65 |
| T-108 | 8(1) | 12(1) | 24(2) | 2.60 | 2.66 |
| T-109 | 8(1) | 12(1) | 24(2) | 2.44 | 3.13 |
| T-110 | 8(1) | 12(1) | 24(2) | 2.53 | 3.03 |
| T-111 | 8(1) | 12(1) | 30(3) | 2.70 | 3.03 |
| T-112 | 8(1) | 12(1) | 30(3) | 2.73 | 3.09 |
| T-113 | 8(1) | 12(1) | 30(3) | 2.66 | 3.05 |
| T-114 | 8(1) | 12(1) | 30(3) | 2.72 | 3.07 |
| T-115 | 8(1) | 12(1) | 30(3) | 2.70 | 2.97 |
| T-116 | 8(1) | 15(2) | 18(1) | 3.14 | 3.01 |
| T-117 | 8(1) | 15(2) | 18(1) | 2.64 | 2.99 |
| T-118 | 8(1) | 15(2) | 18(1) | 3.92 | 2.97 |
| T-119 | 8(1) | 15(2) | 18(1) | 2.86 | 2.96 |
| T-120 | 8(1) | 15(2) | 18(1) | 3.14 | 2.97 |
| T-121 | 8(1) | 15(2) | 24(2) | 2.78 | 3.05 |
| T-122 | 8(1) | 15(2) | 24(2) | 2.69 | 3.22 |
| T-123 | 8(1) | 15(2) | 24(2) | 2.69 | 5.36 |
| T-124 | 8(1) | 15(2) | 24(2) | 2.95 | 3.92 |
| T-125 | 8(1) | 15(2) | 24(2) | 2.78 | 2.73 |
| T-126 | 8(1) | 15(2) | 30(3) | 2.69 | 3.23 |
| T-127 | 8(1) | 15(2) | 30(3) | 2.66 | 3.07 |
| T-128 | 8(1) | 15(2) | 30(3) | 2.68 | 3.01 |
| T-129 | 8(1) | 15(2) | 30(3) | 2.73 | 3.35 |
| T-130 | 8(1) | 15(2) | 30(3) | 2.69 | 3.28 |
| T-131 | 8(1) | 18(3) | 18(1) | 2.55 | 3.19 |
| T-132 | 8(1) | 18(3) | 18(1) | 2.53 | 3.56 |
| T-133 | 8(1) | 18(3) | 18(1) | 2.60 | 3.10 |
| T-134 | 8(1) | 18(3) | 18(1) | 2.52 | 2.70 |
| T-135 | 8(1) | 18(3) | 18(1) | 2.55 | 2.97 |
| T-136 | 8(1) | 18(3) | 24(2) | 2.65 | 3.10 |
| T-137 | 8(1) | 18(3) | 24(2) | 2.58 | 2.98 |
| T-138 | 8(1) | 18(3) | 24(2) | 2.68 | 3.11 |
| T-139 | 8(1) | 18(3) | 24(2) | 2.70 | 4.17 |
| T-140 | 8(1) | 18(3) | 24(2) | 2.65 | 3.42 |
| T-141 | 8(1) | 18(3) | 30(3) | 2.67 | 3.03 |
| T-142 | 8(1) | 18(3) | 30(3) | 2.62 | 4.13 |
| T-143 | 8(1) | 18(3) | 30(3) | 2.77 | 3.54 |
| T-144 | 8(1) | 18(3) | 30(3) | 2.62 | 3.56 |
| T-145 | 8(1) | 18(3) | 30(3) | 2.67 | 2.72 |
| T-146 | 10(2) | 12(1) | 18(1) | 3.07 | 6.32 |
| T-147 | 10(2) | 12(1) | 18(1) | 2.64 | 4.13 |
| T-148 | 10(2) | 12(1) | 18(1) | 3.85 | 4.39 |
| T-149 | 10(2) | 12(1) | 18(1) | 2.71 | 3.93 |

**Table 5** (continued)

| Test no. | Injection speed ($cm^3/s$) | Holding time (s) | Cooling time (s) | Length shrinkage (%) | Width shrinkage (%) |
|---|---|---|---|---|---|
| T-150 | 10(2) | 12(1) | 18(1) | 3.07 | 2.92 |
| T-151 | 10(2) | 12(1) | 24(2) | 2.59 | 5.22 |
| T-152 | 10(2) | 12(1) | 24(2) | 2.59 | 4.20 |
| T-153 | 10(2) | 12(1) | 24(2) | 2.61 | 2.34 |
| T-154 | 10(2) | 12(1) | 24(2) | 2.56 | 2.40 |
| T-155 | 10(2) | 12(1) | 24(2) | 2.59 | 2.43 |
| T-156 | 10(2) | 12(1) | 30(3) | 2.71 | 2.20 |
| T-157 | 10(2) | 12(1) | 30(3) | 2.73 | 1.74 |
| T-158 | 10(2) | 12(1) | 30(3) | 2.68 | 4.39 |
| T-159 | 10(2) | 12(1) | 30(3) | 2.72 | 3.06 |
| T-160 | 10(2) | 12(1) | 30(3) | 2.71 | 3.07 |
| T-161 | 10(2) | 15(2) | 18(1) | 2.67 | 3.87 |
| T-162 | 10(2) | 15(2) | 18(1) | 2.66 | 4.27 |
| T-163 | 10(2) | 15(2) | 18(1) | 2.70 | 3.97 |
| T-164 | 10(2) | 15(2) | 18(1) | 2.66 | 4.13 |
| T-165 | 10(2) | 15(2) | 18(1) | 2.67 | 2.18 |
| T-166 | 10(2) | 15(2) | 24(2) | 2.51 | 3.46 |
| T-167 | 10(2) | 15(2) | 24(2) | 2.62 | 4.27 |
| T-168 | 10(2) | 15(2) | 24(2) | 2.62 | 4.08 |
| T-169 | 10(2) | 15(2) | 24(2) | 2.28 | 4.30 |
| T-170 | 10(2) | 15(2) | 24(2) | 2.51 | 3.35 |
| T-171 | 10(2) | 15(2) | 30(3) | 2.93 | 4.27 |
| T-172 | 10(2) | 15(2) | 30(3) | 3.36 | 3.36 |
| T-173 | 10(2) | 15(2) | 30(3) | 2.66 | 3.17 |
| T-174 | 10(2) | 15(2) | 30(3) | 2.78 | 2.93 |
| T-175 | 10(2) | 15(2) | 30(3) | 2.93 | 3.14 |
| T-176 | 10(2) | 18(3) | 18(1) | 2.76 | 2.57 |
| T-177 | 10(2) | 18(3) | 18(1) | 2.62 | 3.43 |
| T-178 | 10(2) | 18(3) | 18(1) | 2.57 | 3.36 |
| T-179 | 10(2) | 18(3) | 18(1) | 2.89 | 4.66 |
| T-180 | 10(2) | 18(3) | 18(1) | 2.93 | 4.70 |
| T-181 | 10(2) | 18(3) | 24(2) | 3.30 | 2.43 |
| T-182 | 10(2) | 18(3) | 24(2) | 3.73 | 2.70 |
| T-183 | 10(2) | 18(3) | 24(2) | 2.89 | 2.64 |
| T-184 | 10(2) | 18(3) | 24(2) | 2.92 | 2.49 |
| T-185 | 10(2) | 18(3) | 24(2) | 2.86 | 2.56 |
| T-186 | 10(2) | 18(3) | 30(3) | 2.55 | 2.85 |
| T-187 | 10(2) | 18(3) | 30(3) | 2.63 | 3.28 |
| T-188 | 10(2) | 18(3) | 30(3) | 2.64 | 2.73 |
| T-189 | 10(2) | 18(3) | 30(3) | 2.67 | 4.70 |
| T-190 | 10(2) | 18(3) | 30(3) | 2.51 | 3.05 |
| T-191 | 12(3) | 12(1) | 18(1) | 2.69 | 4.17 |
| T-192 | 12(3) | 12(1) | 18(1) | 2.71 | 4.25 |
| T-193 | 12(3) | 12(1) | 18(1) | 2.70 | 2.70 |
| T-194 | 12(3) | 12(1) | 18(1) | 2.70 | 2.59 |
| T-195 | 12(3) | 12(1) | 18(1) | 2.67 | 2.63 |
| T-196 | 12(3) | 12(1) | 24(2) | 2.61 | 2.57 |
| T-197 | 12(3) | 12(1) | 24(2) | 2.61 | 4.55 |
| T-198 | 12(3) | 12(1) | 24(2) | 2.69 | 4.27 |

**Table 5** (continued)

| Test no. | Injection speed ($cm^3/s$) | Holding time (s) | Cooling time (s) | Length shrinkage (%) | Width shrinkage (%) |
|---|---|---|---|---|---|
| T-199 | 12(3) | 12(1) | 24(2) | 2.67 | 4.68 |
| T-200 | 12(3) | 12(1) | 24(2) | 2.69 | 4.16 |
| T-201 | 12(3) | 12(1) | 30(3) | 2.64 | 2.85 |
| T-202 | 12(3) | 12(1) | 30(3) | 2.63 | 3.36 |
| T-203 | 12(3) | 12(1) | 30(3) | 3.08 | 2.57 |
| T-204 | 12(3) | 12(1) | 30(3) | 2.63 | 2.63 |
| T-205 | 12(3) | 12(1) | 30(3) | 2.26 | 4.04 |
| T-206 | 12(3) | 15(2) | 18(1) | 2.80 | 4.63 |
| T-207 | 12(3) | 15(2) | 18(1) | 2.80 | 3.56 |
| T-208 | 12(3) | 15(2) | 18(1) | 2.65 | 3.94 |
| T-209 | 12(3) | 15(2) | 18(1) | 2.59 | 3.35 |
| T-210 | 12(3) | 15(2) | 18(1) | 2.95 | 3.36 |
| T-211 | 12(3) | 15(2) | 24(2) | 2.79 | 4.27 |
| T-212 | 12(3) | 15(2) | 24(2) | 2.64 | 4.47 |
| T-213 | 12(3) | 15(2) | 24(2) | 2.69 | 4.18 |
| T-214 | 12(3) | 15(2) | 24(2) | 2.75 | 3.72 |
| T-215 | 12(3) | 15(2) | 24(2) | 3.07 | 2.22 |
| T-216 | 12(3) | 15(2) | 30(3) | 2.65 | 3.75 |
| T-217 | 12(3) | 15(2) | 30(3) | 2.72 | 4.30 |
| T-218 | 12(3) | 15(2) | 30(3) | 2.59 | 3.01 |
| T-219 | 12(3) | 15(2) | 30(3) | 2.66 | 2.10 |
| T-220 | 12(3) | 15(2) | 30(3) | 2.66 | 2.01 |
| T-221 | 12(3) | 18(3) | 18(1) | 2.65 | 2.57 |
| T-222 | 12(3) | 18(3) | 18(1) | 2.54 | 3.10 |
| T-223 | 12(3) | 18(3) | 18(1) | 2.68 | 2.96 |
| T-224 | 12(3) | 18(3) | 18(1) | 2.72 | 3.48 |
| T-225 | 12(3) | 18(3) | 18(1) | 2.65 | 2.81 |
| T-226 | 12(3) | 18(3) | 24(2) | 2.75 | 3.36 |
| T-227 | 12(3) | 18(3) | 24(2) | 2.78 | 3.01 |
| T-228 | 12(3) | 18(3) | 24(2) | 2.59 | 2.76 |
| T-229 | 12(3) | 18(3) | 24(2) | 2.90 | 3.35 |
| T-230 | 12(3) | 18(3) | 24(2) | 2.76 | 3.23 |
| T-231 | 12(3) | 18(3) | 30(3) | 2.79 | 3.01 |
| T-232 | 12(3) | 18(3) | 30(3) | 2.91 | 2.99 |
| T-233 | 12(3) | 18(3) | 30(3) | 2.82 | 3.05 |
| T-234 | 12(3) | 18(3) | 30(3) | 2.63 | 3.23 |
| T-235 | 12(3) | 18(3) | 30(3) | 2.79 | 2.22 |

## References


1. Han, S., Wang, K.K.: Shrinkage prediction for slowly-crystallizing thermoplastic polymers in injection molding. Int. Polym. Proc. **12**(3), 228–237 (1997)
2. Jansen, K.M.B., Van Dijk, D.J., Husselman, M.H.: Effect of processing conditions on shrinkage in injection molding. Polym. Eng. Sci. **38**(5), 838–846 (1998)
3. Choi, D.S., Im, Y.T.: Prediction of shrinkage and warpage in consideration of residual stress in integrated simulation of injection molding. Compos. Struct. **47**(1), 655–665 (1999)
4. Lucyshyn, T., Knapp, G., Kipperer, M., Holzer, C.: Determination of the transition temperature at different cooling rates and its influence on prediction of shrinkage and warpage in injection molding simulation. J. Appl. Polym. Sci. **123**(2), 1162–1168 (2012)
5. Pomerleau, J., Sanschagrin, B.: Injection molding shrinkage of PP: experimental progress. Polym. Eng. Sci. **46**(9), 1275–1283 (2006)
6. Shen, C., Wang, L., Li, Q.: Optimization of injection molding process parameters using combination of artificial neural network and genetic algorithm method. J. Mater. Process. Technol. **183**(2), 412–418 (2007)
7. Lee, S.C., Youn, J.R.: Shrinkage analysis of molded parts using neural network. J. Reinf. Plast. Compos. **18**(2), 186–195 (1999)

8. Liao, S.J., Hsieh, W.H., Wang, J.T., Su, Y.C.: Shrinkage and warpage prediction of injection-molded thin-wall parts using artificial neural networks. Polym. Eng. Sci. **44**(11), 2029–2040 (2004)
9. Wang, R., Zeng, J., Feng, X., Xia, Y.: Evaluation of effect of plastic injection molding process parameters on shrinkage based on neural network simulation. J. Macromol. Sci. Part B **52**(1), 206–221 (2013)
10. Altan, M.: Reducing shrinkage in injection moldings via the Taguchi, ANOVA and neural network methods. Mater. Des. **31**(1), 599–604 (2010)
11. Tsai, K.M., Luo, H.J.: An inverse model for injection molding of optical lens using artificial neural network coupled with genetic algorithm. J. Intell. Manuf. **28**(2), 473–487 (2017)
12. Gong, G., Chen, J.C., Guo, G.: Enhancing tensile strength of injection molded fiber reinforced composites using the Taguchi-based six sigma approach. Int. J. Adv. Manuf. Technol. **91**(9), 3385–3393 (2017)
13. Chang, T.C., Faison, E.: Shrinkage behavior and optimization of injection molded parts studied by the Taguchi method. Polym. Eng. Sci. **41**(5), 703–710 (2001)
14. Demuth, H. and Beale, M., 1992. Neural Network Toolbox. *For Use with MATLAB. The MathWorks Inc*, *2000*

**Publisher's Note** Springer Nature remains neutral with regard to jurisdictional claims in published maps and institutional affiliations.